Cell Stem Cell
Article

Induction of Multipotential Hematopoietic Progenitors from Human Pluripotent Stem Cells via Respecification of Lineage-Restricted Precursors

Sergei Doulatov,[1,2] Linda T. Vo,[1,2] Stephanie S. Chou,[1,2] Peter G. Kim,[1,2] Natasha Arora,[1,2] Hu Li,[3,4] Brandon K. Hadland,[5,6] Irwin D. Bernstein,[5,6] James J. Collins,[3,4] Leonard I. Zon,[2,7,8] and George Q. Daley[1,2,8,*]
[1]Stem Cell Transplantation Program, Division of Pediatric Hematology/Oncology, Manton Center for Orphan Disease Research, Howard Hughes Medical Institute, Children's Hospital Boston and Dana Farber Cancer Institute; Department of Biological Chemistry and Molecular Pharmacology, Harvard Medical School, Boston, MA 02115, USA
[2]Harvard Stem Cell Institute, Cambridge, MA 02138, USA
[3]Howard Hughes Medical Institute, Department of Biomedical Engineering and Center for BioDynamics, Boston University, Boston, MA 02215, USA
[4]Wyss Institute for Biologically Inspired Engineering, Harvard University, Boston, MA 02115, USA
[5]Clinical Research Division, Fred Hutchinson Cancer Research Center, Seattle, WA 98109, USA
[6]Department of Pediatrics, University of Washington, Seattle, WA 98105, USA
[7]Stem Cell Program, Division of Pediatric Hematology/Oncology, Children's Hospital Boston, Howard Hughes Medical Institute, Boston, MA 02115, USA
[8]Broad Institute, Cambridge, MA 02141 USA
*Correspondence: george.daley@childrens.harvard.edu
http://dx.doi.org/10.1016/j.stem.2013.09.002

SUMMARY

Human pluripotent stem cells (hPSCs) represent a promising source of patient-specific cells for disease modeling, drug screens, and cellular therapies. However, the inability to derive engraftable human hematopoietic stem and progenitor cells (HSPCs) has limited their characterization to in vitro assays. We report a strategy to respecify lineage-restricted $CD34^+CD45^+$ myeloid precursors derived from hPSCs into multilineage progenitors that can be expanded in vitro and engrafted in vivo. HOXA9, ERG, and RORA conferred self-renewal and multilineage potential in vitro and maintained primitive $CD34^+CD38^-$ cells. Screening cells via transplantation revealed that two additional factors, SOX4 and MYB, conferred engraftment. Progenitors specified with all five factors gave rise to reproducible short-term engraftment with myeloid and erythroid lineages. Erythroid precursors underwent hemoglobin switching in vivo, silencing embryonic and activating adult globin expression. Our combinatorial screening approach establishes a strategy for obtaining transcription-factor-mediated engraftment of blood progenitors from human pluripotent cells.

INTRODUCTION

Recent advances in reprogramming to induced pluripotent stem cells (IPSCs) have provided access to a wide array of patient-specific pluripotent lines that have the potential to give rise to any somatic cell type. A large number of pluripotent lines have been generated from patients with hematologic diseases, including Fanconi anemia (Müller et al., 2012), sickle cell anemia (Zou et al., 2011), Diamond Blackfan anemia (Garçon et al., 2013), Shwachman Diamond syndrome (Tulpule et al., 2013), chronic myelogenous leukemia (Kumano et al., 2012), $JAK2^{V617F}$ myelo-proliferative disorder (Ye et al., 2009), dyskeratosis congenita (Agarwal et al., 2010), Pearson syndrome (Cherry et al., 2013), and others. These lines have the potential to become powerful models to gain insight into the molecular basis of disease and platforms for drug screens (Cherry and Daley, 2013). To reveal the disease phenotype, IPSCs have to be differentiated into the target cell type of interest—hematopoietic stem and progenitor cells (HSPCs). Numerous protocols for hematopoietic differentiation of hPSCs into short-lived progenitors and mature cells have been established (Chadwick et al., 2003; Kennedy et al., 2012). However, no system presently exists to generate large numbers of transplantable cells from human pluripotent stem cells (hPSCs), thereby precluding disease modeling in vivo and hampering the scope of experiments and screens that can be performed.

A major hurdle for generating engraftable HSPCs is the complex nature of hematopoietic ontogeny. It is now widely accepted that hematopoietic cells arise during midgestation in multiple temporal waves from hemogenic endothelial (HE) cells lining the major arteries (Bertrand et al., 2010; Boisset et al., 2010). Directed differentiation protocols attempt to recapitulate ontogeny by calibrated addition of morphogens such as BMP4, Activin A, and Notch ligands. These protocols can promote the emergence of HE cells and recapitulate the temporal waves of hematopoietic progenitors, but they generate few if any transplantable cells (Choi et al., 2012; Kennedy et al., 2012). Prior reports of limited engraftment of hPSC-derived cells in immunodeficient mice have not been widely exploited owing to the heterogeneity among hPSC lines and variations among protocols (Ledran et al., 2008; Wang et al., 2005). More importantly, these protocols generate only small numbers of transplantable cells, and without the possibility of expanding them,

it is difficult to move toward more practical models, such as in vivo engraftment of disease IPSCs.

One approach that has not been extensively explored in hematopoietic development is transcription-factor-mediated specification and expansion of HSPCs. It was recently shown that a combination of Gata2, Gfi1b, Fos, and Etv6 promotes conversion of mouse fibroblasts into hematopoietic cells, suggesting that transcription factor reprogramming is a promising approach (Pereira et al., 2013). However, since fibroblasts are a distinct cell type, the precise conversion to HSPCs remains a challenge. We propose that conversions from closely related lineages, which minimize the "epigenetic distance" to a desired cell type, provide a more favorable context for precise alterations in cell fate. One possible approach is to promote specification of HE into transplantable HSPCs, which takes advantage of normal developmental cues. However, the process of endothelial to hematopoietic transition remains poorly understood, making it difficult to design rational interventions. An alternative approach is to start with committed hematopoietic progenitors and revert them to a more immature state. Such "respecification" combines directed differentiation with transcription-based reprogramming to establish HSPC fate. A logical hypothesis is that the key regulatory factors that maintain HSCs can reactivate stem cell properties, such as self-renewal, in more mature progenitors. Molecular differences between primary human HSCs and progenitors have been well characterized by gene expression profiling, thereby enabling a rational approach to introduce candidate stem cell genes back into progenitors (Doulatov et al., 2010; Laurenti et al., 2013).

Respecification was likely first demonstrated in mouse embryonic stem cells (ESCs) using the homeobox transcription factor HoxB4. Expression of HoxB4 in lineage-restricted hematopoietic progenitors isolated from embryoid body (EB) differentiation or from yolk sac endowed them with extended self-renewal and long-term multilineage engraftment capacity (Kyba et al., 2002). HOXB4 has not functioned similarly in human ESCs (Lee et al., 2008; Wang et al., 2005) or HSCs (Amsellem et al., 2003), suggesting species-specific differences. These studies, however, prompted us to search for factors tailored for hPSCs. Here, we identify HOX- and ETS-family transcription factors HOXA9 and ERG as inducers of self-renewal and multilineage potential in hematopoietic progenitors differentiated from hPSCs. The addition of SOX4 and MYB modulates this network to enable myeloid and erythroid engraftment, paving the way for in vivo models of hematological diseases from human IPSCs.

RESULTS

Selection of Candidate Transcription Factors

We hypothesized that introduction of stem cell transcription factors into hematopoietic progenitors derived from hPSCs would endow these cells with stem cell properties such as self-renewal potential. Gene expression of purified mouse and human HSCs has been extensively analyzed. Since functionally relevant factors are likely conserved, we used two independent mouse (Chambers et al., 2007; Ivanova et al., 2002) and two human (Doulatov et al., 2010; Novershtern et al., 2011) data sets to select transcriptional regulators more highly expressed in HSCs compared with progenitors or mature cells. Factors enriched in either of the two species-specific data sets were intersected to identify conserved regulators. These were then compared with gene sets differentially regulated during ontogeny to select factors upregulated in definitive HSCs (McKinney-Freeman et al., 2012). From this list of 32 HSC-specific transcription factors, 9 are significantly underexpressed in $CD34^+CD45^+$ EB progenitors compared with $CD34^+CD38^-$ cord blood (CB) HSCs (Wang et al., 2005). These are *ERG*, *KLF4*, *SOX4*, *MYB*, *RORA*, *HLF*, *HOXA5*, *HOXA9*, and *HOXA10*. These open reading frames were cloned into a pSMAL-GFP lentiviral vector. Lentiviruses were produced as a minilibrary of nine factors (9F), plus luciferase (LUC), which serves as an internal control (Figure S1A available online).

An In Vitro Screen for Self-Renewal Capacity

To generate hematopoietic progenitors, hPSCs were differentiated as EBs in the presence of BMP4 and cytokines, as previously described (Chadwick et al., 2003). An ESC line, CHB6, and an IPSC line, MSC-IPS1, were selected based on their robust hemogenic potential (Figure S1B). In these conditions, $CD34^+CD45^+$ progenitors appear at day 10 and expand until day 14 (Figure 1A). Since EBs in our protocol are cultured with serum, the day 14 progenitors likely represent a mixture of primitive and definitive cell types (Figure S1C). Progenitors isolated by flow sorting at day 14 possess robust myeloid colony-forming activity, but produce few erythroid or mixed colonies (Figure 1B). When cultured in serum-free media with cytokines, they rapidly differentiate and lose this potential, and after 7 days in culture no colonies are ever observed, indicating a complete lack of proliferative and self-renewing potential (Figure 1B). We reasoned that if a combination of factors allowed progenitors to proliferate and undergo self-renewal divisions—a basic property of HSCs—these would appear as rare colonies after extended culture. To test the candidate transcription factors in this simple screen, $CD34^+CD45^+$ progenitors were infected with the 9F library, cultured for 7 days, and plated in colony assays. Both CHB6 and MSC-IPS1 progenitors infected with 9F, but not *LUC* alone, consistently gave rise to colonies in independent experiments (Figure 1C). Single colonies were isolated and analyzed for the presence of integrated viral transgenes (Figure 1D). The frequency of *LUC* integrations controlled for infection efficiency, with more frequent integrations being under positive selection. Each colony harbored four to eight integrations, with *HLF*, *ERG*, *HOXA9*, and *RORA* present in almost every colony. In an independent experiment with a lower transduction efficiency, *HOXA9* and *RORA* were also under selection (Figure S1D). The colony-forming capacity could be sustained for at least 3 weeks in culture (Figure 1E). To further investigate this renewal potential, we carried out serial replating. Some, but not all, 9F-infected replicates had robust replating potential (Figure 1F). Almost all colonies from the replicates with high replating potential had *HLF*, *ERG*, *HOXA9*, and *RORA* integrations. By contrast, colonies from the poorly replating replicates harbored fewer integrations (Figure 1G) suggesting that higher-order combinations were important.

Retrospective analysis has identified HLF, ERG, HOXA9, and RORA as candidate factors that endow embryonic hematopoietic progenitors with self-renewal capacity. To test them

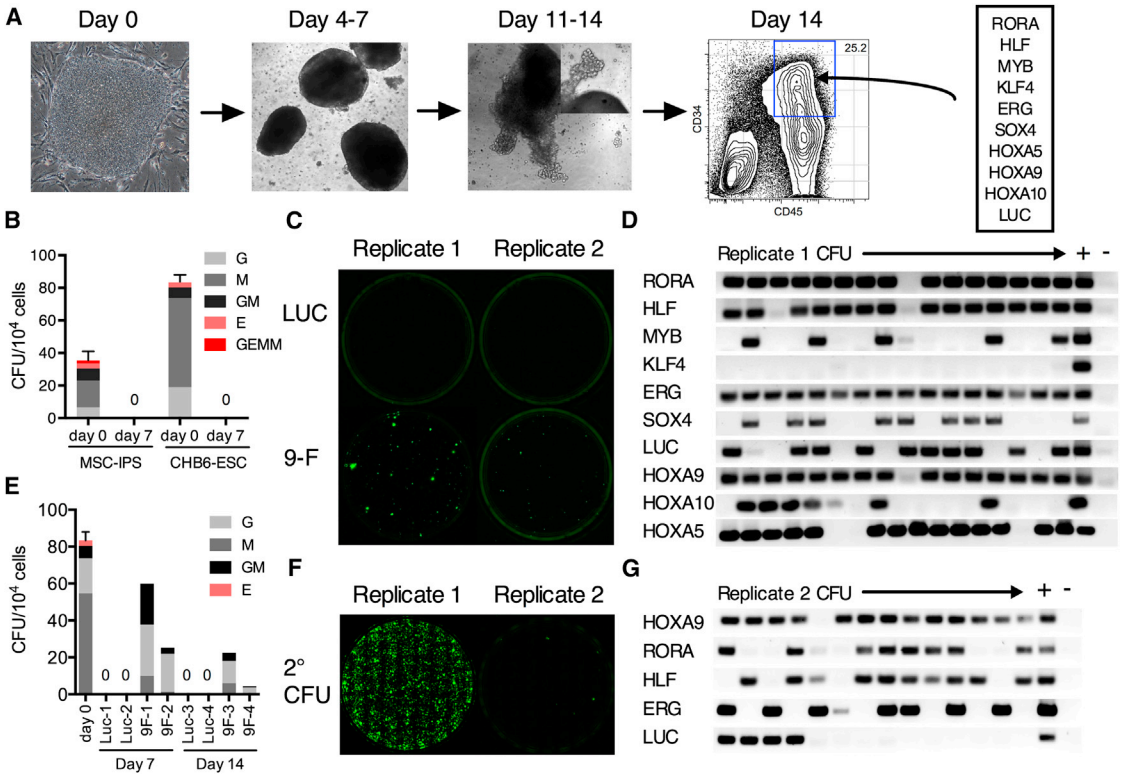

Figure 1. In Vitro Screen for Progenitor Respecification

(A) The scheme for EB differentiation of hPSCs into hematopoietic progenitors. EBs cultured in serum, BMP4, and cytokines are dissociated after 14 days. $CD34^+CD45^+$ progenitors are isolated by flow sorting and transduced with a 9F lentiviral library.

(B) Colony-forming capacity of $CD34^+CD45^+$ EB progenitors from MSC-IPS1 and CHB6-ESC after sorting (day 0) is lost after 7 days of culture in serum-free media.

(C) Representative plates of CHB6 EB progenitors transduced with the 9F library showing emergence of de novo hematopoietic colonies after 7 days of culture.

(D) Retrospective analysis of transgene insertions in individual colonies isolated from replicate #1 in (C). LUC is an internal control for transduction efficiency. Columns "+" and "–" are positive and negative controls for PCR.

(E) Colony counts and types observed after 7 or 14 days of culture of luciferase (Luc) or 9F-transduced progenitors.

(F) Serial replating potential of 9F replicates.

(G) Transgene insertions for a nonreplating sample (replicate #2 in C) show that most colonies do not contain higher-order combinations of the common integrations.

Data are shown as mean ± SEM of three independent samples. See also Figure S1.

prospectively, we infected $CD34^+CD45^+$ cells with all 16 combinations of the four factors and assayed each by plating colonies at day 7 of culture. Rare colonies appeared in single *ERG*- or *HOXA9*-transduced samples, but both *ERG* and *HOXA9* (abbreviated "*EA*") were required for robust colony-forming activity in both CHB6 and MSC-IPS1 progenitors (Figures 2A–2C and Figures S2A and S2B). The addition of *RORA* (abbreviated "*EAR*") enhanced colony formation, while addition of *HLF* did not alter the number of colonies for any combination of factors (Figure 2B). *EA* colonies were larger in size, whereas *EAR* specified more colonies. Consistent with this, *EA* cultures proliferated more rapidly than *EAR*, which contained more progenitors with slower cell cycle kinetics (Figures 2D and 2E). No colonies were observed in any single-infected samples after 14 days of culture. *ERG* or *HOXA9* single-transduced samples also never gave rise to secondary colonies, implying that multiple factors are required for respecification. By contrast, most of the *EAR*-transduced replicates could be serially replated (Figures 2B, S2A, and S2B). Based on these data we included *RORA* in subsequent experiments.

Our data suggest that activation of self-renewal in hPSC-derived progenitors requires at least two transcription factors—HOXA9 and ERG. Notably, *EA* also promoted renewal of CB $CD34^+$ progenitors in vitro, and the possibility of respecifying adult progenitors to HSPCs warrants further exploration (Figure S2C). HOXA9 is the key homeotic gene that defines HSPC identity (Di-Poï et al., 2010; Lawrence et al., 2005). ERG is a component of HSC renewal during embryogenesis and stress hematopoiesis (Loughran et al., 2008). *ERG* is also a transcriptional target of HOXA9, suggesting a basis for their functional cooperation in our assay (Huang et al., 2012).

HOXA9, ERG, and RORA Establish a Hematopoietic Hierarchy

Individual lineages in the hematopoietic hierarchy can be accurately distinguished by a combination of cell surface antigens.

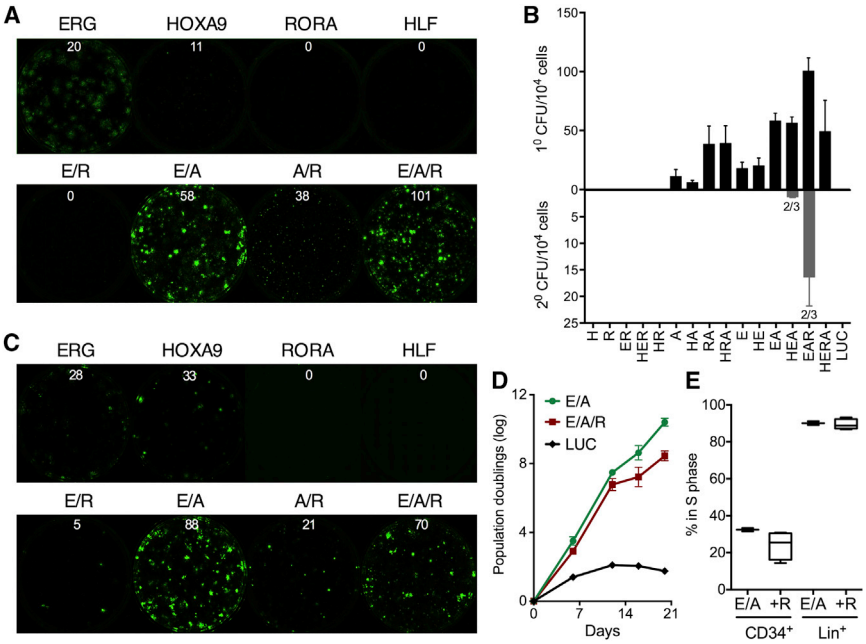

Figure 2. Self-Renewal Is Driven by HOXA9, ERG, and RORA

(A–C) Prospective analysis of HOXA9 (A), ERG (E), HLF (H), and RORA (R) combinations in CHB-ESC (A and B) and MSC-IPS1 (C) (see also Figure S2A) progenitors using the in vitro colony assay. Independent pluripotent lines are shown to demonstrate reproducibility of the factor combinations. Representative plates for combinations of HOXA9, ERG, and RORA are shown in (A) and (C), and the full quantitation of primary and secondary colony-forming efficiency is shown in (B). Numbers above the plates indicate an average number of colonies per 10^4 cells plated. Numbers below secondary bars indicate the fraction of replicates that gave rise to secondary colonies.

(D) Proliferation of ERG, HOXA9, and RORA (*EAR*)-transduced progenitors compared with ERG and HOXA9 without RORA (*EA*) and LUC control.

(E) Cell cycle analysis of *EA*- and *EAR*-induced $CD34^+$ cells and the more mature lineage-positive (Lin^+; defined as $CD14^+$, $CD15^+$, or $CD11b^+$) cells with or without RORA after 14 days of culture.

All data are shown as mean ± SEM of at least three independent replicates. See also Figure S2.

We next examined if *EAR*-induced hematopoiesis generated progenitor subsets that resemble those found in CB or adult marrow. Cultured EB $CD34^+CD45^+$ progenitors completely differentiate into $CD34^-$ cells after 7 days of culture, which is consistent with loss of clonogenic capacity (Figure 3A). By contrast, a $CD34^+$ population was maintained in *EAR* cultures, expanding between 7 to 14 days, and persisting after that (Figure 3A). $CD34^+$ cells were also found in dissociated primary colonies, accounting for serial replating. CD34 expression segregated with the lineage-negative population that did not express myeloid markers CD14, CD15, or CD11b. Human HSCs are found exclusively in the $CD34^+CD38^-$ compartment, and the loss of stem cell potential is correlated with the gradual acquisition of CD38 and loss of CD34 expression (Mazurier et al., 2003). The starting EBs lack a clearly defined $CD34^+CD38^-$ population (Figure 3B). By contrast, *EAR* established a pattern of CD34 and CD38 closely resembling that of lineage-depleted CB (Figure 3B). $CD90^+CD49f^+$ cells could be further identified within the $CD34^+CD38^-$ *EAR* compartment, which is highly enriched for HSCs in CB (Figure 3B) (Notta et al., 2011). Thus, the three factors establish a rudimentary HSPC hierarchy, even in the presence of constitutive transgene expression.

HOXA9, ERG, and RORA Reactivate Expression of HSC Genes

To clarify the molecular basis for self-renewal of respecified progenitors, we performed microarray profiling of $CD34^+CD38^-$ cells isolated by flow sorting from EBs, *EAR* cultures, and primary $CD34^+CD38^-$ HSCs and $CD34^+CD38^+$ progenitors from CB and fetal liver (FL). Unsupervised clustering showed that these populations segregated to distinct branches, indicating broad differences in gene expression (Figure 4A). To define the molecular program initiated by the factors, we identified genes induced or repressed greater than 2-fold by *EAR* in EB progenitors (t test, FDR < 0.05; Table S1 available online). The majority of these 2,070 genes were concordantly expressed in HSCs (Figure 4B), including genes on in HSCs activated by *EAR* (group A) and genes off in HSCs repressed by *EAR* (group C). The transcription factors induced by *EAR* include *RUNX1*, *HLF*, the AP-1 family (*FOS*, *JUN, MAFF*), and *GFI1B*, all critical elements of a normal HSC program (Figure 4B). To analyze this using a different metric, we employed refined signatures for the human HSPC hierarchy (Laurenti et al., 2013). Six signatures capture the major patterns of early transcription: HSC, MLP (early lymphoid), HSC_MLP (shared stem and lymphoid), GMP (myeloid), CMP_MEP (erythroid), and Progenitor (shared between all progenitors). HSC and HSC_MLP signatures were significantly enriched in *EAR* compared to EBs (Figure 4C, bottom row). By contrast, progenitor signatures were enriched in EBs (Figure 4C, top row). These data show that while factor-transduced progenitors retain similarity to EBs, *EAR* initiates a gene expression program that is shared with normal HSCs.

To further analyze transcriptional changes induced by the three factors, we performed gene-set enrichment analysis for annotated gene sets in the MSigDB database. HSC gene sets and HOXA9 targets were enriched in *EAR*, while cell cycle, serum response, and oncogene-induced gene sets were enriched in EBs (Figure S3A). To test if the factors turn on some HSC-specific genes and repress progenitor-specific genes, we compiled a list of genes differentially expressed between CB/FL HSCs and progenitors (t test, FDR < 0.05; Table S2). Genes on in HSCs were largely off in EBs, indicating a loss of stem cell gene expression. *EAR* activated some of these genes, although the trend did not reach significance (Figure S3B). This was mirrored by HSC-specific transcription factors, most of which were underexpressed in EB progenitors (Figures 4D and 4E). We discerned two patterns of expression in response to *EAR*: factors reactivated by *EAR* to levels similar in HSCs, including *HLF*, *NFIB*, *HOPX*, *HMGA2*, and *RBPMS* (Figure 4D), and transcription factors not affected by *EAR*, such as *GATA3*,

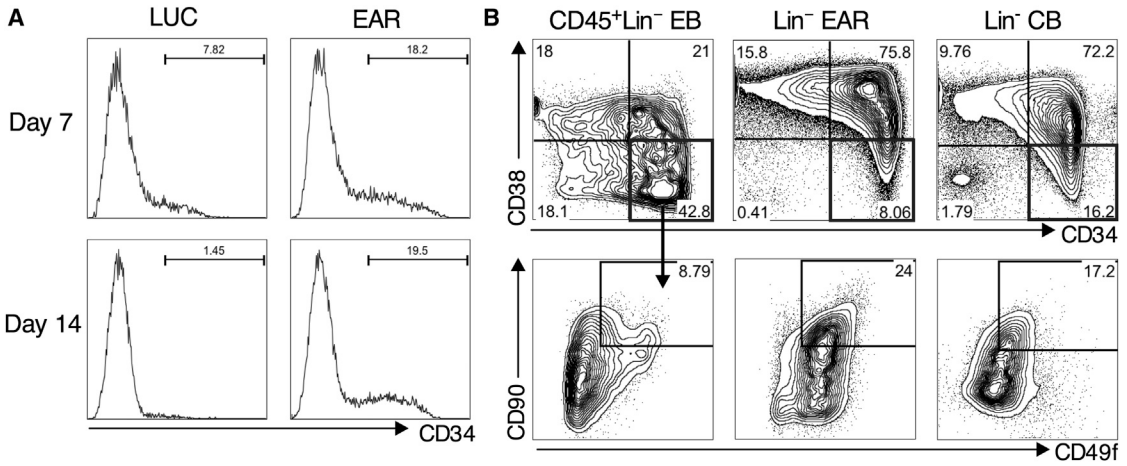

Figure 3. Factor-Based Establishment of Hematopoietic Hierarchy

(A) Progressive loss of $CD34^+$ progenitors in control serum-free cultures (LUC) while *EAR* maintains and expands $CD34^+$ cells (right panels).

(B) Detailed analysis of the phenotypic HSC compartment in EBs, *EAR* cultures (from dissociated colonies), and primary CB. Lineage-positive cells are gated out (using a combination of CD14/CD15/CD11b for EBs and *EAR*). CD34 and CD38 delineates $CD34^+CD38^-$ HSCs and $CD34^+CD38^+$ progenitors (top). $CD34^+CD38^-$ fraction is further marked by CD90 and CD49f (bottom) with double positive cells being the most primitive in CB.

PRDM16, *EVI1*, *MLLT3*, and *NKX2-3* (Figure 4E). HOXA9 cofactors *MEIS1* and *PBX1* also belonged to this group. Genes off in HSCs and on in progenitors, including myeloid and erythroid transcription factors, such as *GATA1*, *KLF1*, *LEF1*, *CEBPA*, and *MITF*, were highly expressed in EBs and significantly downregulated by *EAR* (Figures 4F and S3B). These data suggest that EB progenitors lack the functional properties of HSCs not only because they fail to upregulate HSC-specific genes, but also because they express negative regulators of stem cell function that define differentiated cells (see Table S3 for EB versus HSC gene list). While respecified progenitors remain different from HSCs (see Table S4 for *EAR* versus HSC gene list), *EAR* upregulated a subset of HSC-specific genes and repressed progenitor genes, which likely accounts for their capacity to induce self-renewal in progenitors.

In Vivo Engraftment Requires SOX4 and MYB

We next tested if transcription-factor-respecified progenitors can successfully engraft in irradiated mice. After 2 weeks of primary culture, 1×10^6 *EAR* cells were transplanted into NOD/SCID-IL2Rγnull (NSG) mice. We found no detectable human engraftment 4 weeks after transplant using two independent CD45 antibodies to accurately detect human chimerism (n = 10). This indicated that either *EAR* was insufficient for even short-term engraftment or that changes induced during culture impaired their capacity for homing and retention in the bone marrow. At the same time, we also transplanted 9F library-transduced progenitors. One mouse that had received a transplant into the right femur had a 0.2% human engraftment after 4 weeks (Figure 5A). The integration pattern in $CD45^+$ cells isolated by flow sorting showed the presence of *SOX4* and *MYB* transgenes in addition to *EAR* (Figure 5A). This finding suggested that different transgenes were selected during in vivo reconstitution and led us to believe that the addition of SOX4 and MYB to our cocktail of transcription factors would enable engraftment of EB-derived progenitors.

Transcription Factors Respecify Myeloid-Restricted Precursors into Multilineage Progenitors

To investigate the functional outcome of combining SOX4 and MYB with HOXA9, ERG, and RORA (*EARSM*), we infected $CD34^+CD45^+$ progenitors as before and carried out colony assays after 14 days of culture. While *EAR* gave rise to only myeloid colonies, the addition of *SOX4* and *MYB* prompted the appearance of a large number of blast erythroid (BFU-E) and mixed myelo-erythroid (CFU-GEMM) colonies (Figure 5B). The appearance of GEMM colonies was notable since these are typically not detected, or very rare, among $CD34^+CD45^+$ EB progenitors. Mixed colonies contained both $CD11b^+$ myeloid and $CD235a^+$ erythroid cells. Myelo-erythroid cells were only found in the GFP^- fraction, whereas GFP^+ cells were $CD11b^+$ or $CD34^+$ (Figure 5C), suggesting that erythroid potential was only realized upon transgene silencing.

To explore this possibility, we switched to an inducible lentiviral system in which rtTA is expressed from the same vector as the transgene (Meerbrey et al., 2011). Progenitors were infected with five inducible lentiviruses and cultured in doxycycline (Dox) before colonies were plated with or without Dox. As predicted, GEMM colonies formed only upon Dox withdrawal (Figure 5D). Colonies plated with Dox contained a mixture of $CD11b^+$ cells and $CD34^+$ self-renewing progenitors; rare erythroid cells were always derived from transgene silencing (Figure 5E). Upon Dox withdrawal, $CD34^+$ progenitors differentiated completely into $CD235a^+CD71^+$ erythroid or $CD11b^+$ cells (Figure 5E). Rapid cessation of self-renewal upon Dox withdrawal is explained by the lack of endogenous *HOXA9* and *ERG* transcription, making the system sensitive to induced transgene expression (Figure S4). This presents an attractive system with a high degree of control over self-renewal versus differentiation to model normal and disease hematopoiesis.

Two hypotheses can be put forward to account for the appearance of mixed colonies after factor transduction. One possibility is expansion of the rare GEMM progenitors present

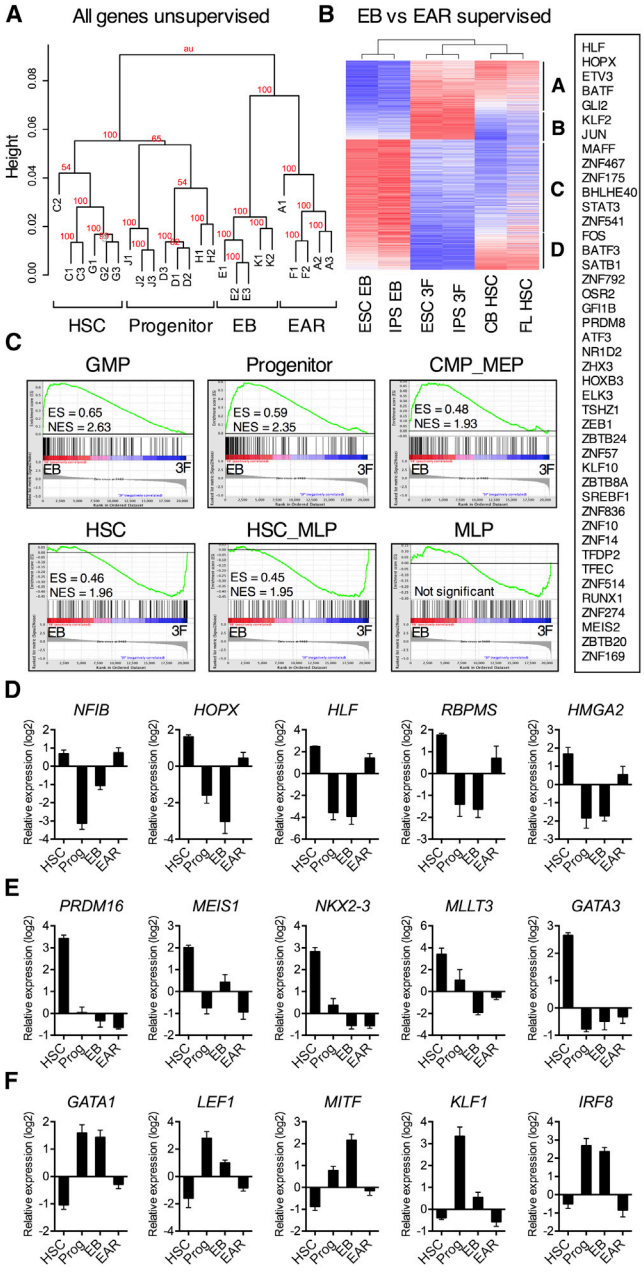

Figure 4. Gene Expression Analysis of Respecified Progenitors

$CD34^+CD38^-$ cells respecified with *EAR* (fractions A and F) were compared to their respective starting CHB6-ESC and MSC-IPSC EBs (fractions E and K), primary CB and FL HSCs (fractions C and G), and $CD34^+CD38^+$ progenitors (fractions D and H) by Affymetrix microarray profiling. Each sample was isolated by flow sorting with two or three biological replicates (#1–3).

(A) Unsupervised global clustering of all probes. Bootstrap values indicate confidence levels.

(B) Supervised clustering of 2,070 genes differentially expressed between $CD34^+CD38^-$ EBs and *EAR* progenitors respecified from them (>2-fold; t test, FDR < 0.05). Clusters of differential genes are marked A–D. Transcription factors significantly upregulated by *EAR* (from clusters A and B) are boxed on the right. See Table S1 for a full list of genes.

(C) Gene set enrichment of human HSC and progenitor signatures in EBs compared with *EAR* progenitors. ES = enrichment score; NES = normalized enrichment score; all comparisons were significant with FDR < 10^{-4}, except MLP.

(D–F) Expression levels of top differentially expressed transcription factors (ranked by fold change) between CB and FL HSCs and progenitors (>2-fold; t test, FDR < 0.05; see Table S2 for a full gene list). Expression values are median transformed relative to all probes. (D) HSC transcription factors significantly upregulated by *EAR*. (E) HSC transcription factors not induced *EAR*. (F) Progenitor transcription factors significantly repressed by *EAR*.

Data are shown as mean ± SEM of six total biological replicates for HSCs, or five replicates for progenitors, EBs, and *EAR*. See also Figure S3, Table S3, and Table S4.

in the day 14 EBs. Due to heterogeneity among hPSC lines, rare GEMM colonies were in fact detected in MSC-IPS1, but not CHB6 EB progenitors (Figure 5F). In stark contrast, the emergence of GEMM colonies after *EARSM* transduction was efficient (up to 25% of all colonies) and highly reproducible with both CHB6 and MSC-IPS1 lines (Figure 5F). We tested the effect of culture on immobilized Delta1, which has been shown to support the expansion of HSPCs by providing a low level Notch signal (Delaney et al., 2005). Delta1-cultured progenitors trended toward higher numbers of GEMM colonies, but the trend did not reach significance. To examine this further, we screened a panel of IPSC lines and identified two lines, BJ-IPS1 and CD45-IPS1, derived from normal foreskin fibroblasts and $CD45^+$ peripheral blood cells, respectively, that did not give rise to BFU-E or GEMM colonies (Figure 5F, "Other IPSCs"). Both lines reproducibly gave rise to erythroid and mixed colonies after induction with *EARSM* (Figure 5F). These data argue against the possibility that the factors simply expand progenitors present in the starting EBs and instead suggest that they actively respecify myeloid-restricted precursors to a myelo-erythroid fate.

Lymphoid potential is critical evidence for respecification, since EB progenitors do not generate B or T cells (Martin et al., 2008). To test lymphoid potential, we seeded *EAR*-transduced cells on OP9-DL1 stroma that promotes T cell differentiation. CB $CD34^+$ cells progress through well-defined stages of differentiation, starting with the acquisition of early lymphoid markers CD7 and CD5 and culminating with $CD4^+CD8^+$ lymphocytes. We noted that *EAR* cultures from which Dox was removed failed to proliferate; however, continued exposure to Dox reduced maturation past the $CD7^+$ stage. Cultures in which Dox was added for the first 2 weeks only showed improved maturation, with more than 4% of lymphocytes reaching the $CD4^+CD8^+$ stage after 5 weeks (Figure 5G). Similar frequencies of $CD1a^+$ and $CD3^+$ cells were observed (Figure S5). By comparison, >13% of CB $CD34^+$ cells were $CD4^+CD8^+$ with robust coexpression of CD1a and CD3 (Figures 5G and S5). These data show that factor-induced progenitors harbor lymphoid potential indicative of respecification to a definitive cell type. However, their lymphoid potential is considerably less than that for adult progenitors, and further optimization of transcription factor combinations is needed.

Respecified Progenitors Mediate Short-Term Myeloid and Erythroid Engraftment

The establishment of a robust and reproducible transplantation model from hPSCs is an important goal. To test the engraftment potential of respecified progenitors, we used the inducible transgene system to expand EB-derived progenitors for 14 days with Dox, and transplanted 0.8–1.2 million cells

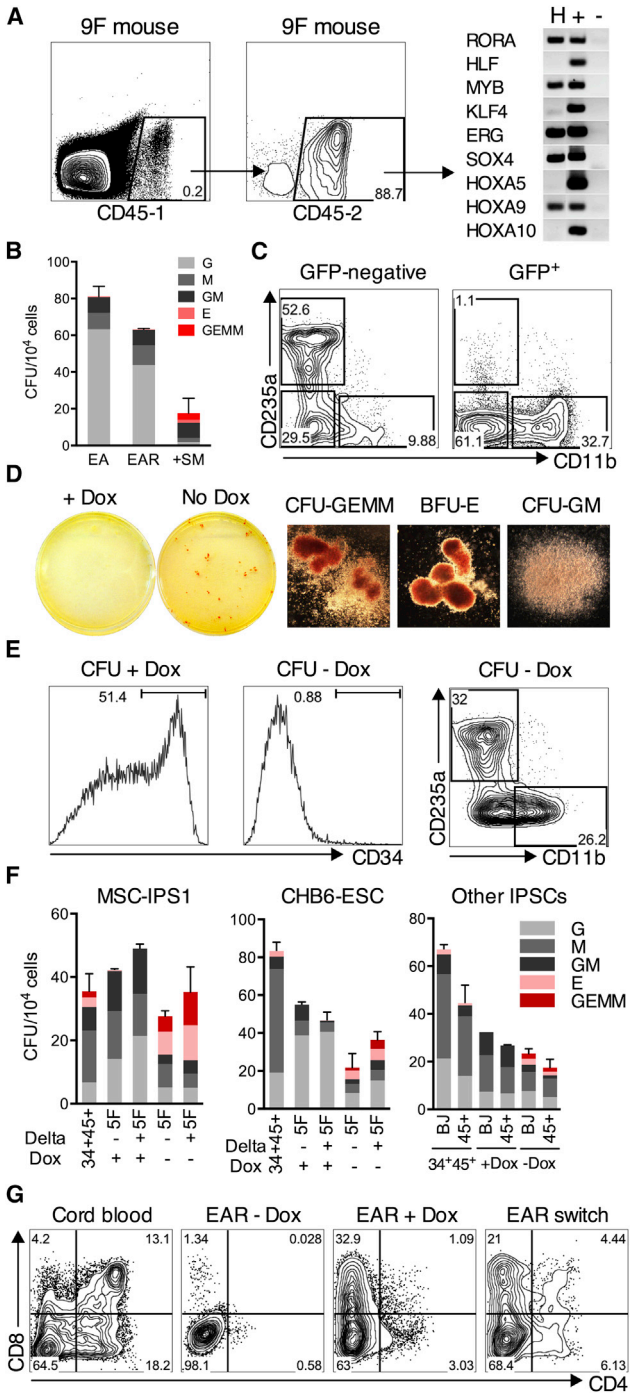

Figure 5. Respecification of Myeloid-Restricted Precursors into Multilineage Progenitors

(A) Detailed analysis of human engraftment in a mouse transplanted with 9F cells after 14 days of culture. Two independent CD45 antibodies (CD45-1 and CD45-2) were used to label human cells. (Right) Transgene insertions in CD45$^+$ cells (column H) isolated from this mouse by flow sorting show SOX4 and MYB integrations.

(B) Colony-forming efficiency of EB progenitors transduced with *EA*, *EAR*, and *EARSM* (+SM) after 14 days of culture.

(C) Flow analysis of dissociated *EARSM* colonies using CD235a (erythroid) and CD11b (myeloid) lineage markers. At least ten GEMM colonies were pooled, and plots are gated on GFP$^+$ or GFP$^-$ populations.

(expanded from <5,000 EB CD34$^+$CD45$^+$ cells) into the femurs of adult NSG mice. Human engraftment was evaluated after 4 or 8 weeks using two human CD45 antibodies, erythroid (CD235a), myeloid (CD33), and lymphoid (CD19, CD5) lineage markers.

Mice transplanted with MSC-IPS1 *EARSM* progenitors were engrafted in the injected femur after 4 weeks, and at lower levels, in the rest of bone marrow (Figure 6A and Figure S6A). We observed only minimal engraftment in mice when Dox was removed (Figure S6B). When Dox was administered, almost all injected mice were engrafted, with an average engraftment across several independent experiments and culture conditions of 2.1% (9 of 12 mice engrafted >0.1%). Similar engraftment levels were observed with CHB6-ESC progenitors (average 0.63%, three of four mice engrafted >0.1%) (Figure 6B). In most recipients, both myeloid and erythroid cells were present; however, in some mice only myeloid or only erythroid engraftment was found (Figure 6C). By contrast with CB-transplanted mice, we did not detect CD19$^+$ B cells. To test the reproducibility of this system using independent IPSC lines, we transplanted *EARSM*-transduced progenitors derived from BJ-IPS and CD45-IPS lines. We observed a similar myelo-erythroid pattern of engraftment in these mice (Figure 6D). In total, 16 of 21 mice transplanted from four hPSC lines were engrafted, with an average engraftment of 2.7% (Figure 6E).

The presence of erythroid engraftment was notable since immunodeficient mice do not robustly support human erythropoiesis (Hu et al., 2011). We observed that several mice with symptoms of radiation sickness—low weight, enlarged spleens, and peripheral lymphocytopenia—had high levels of erythroid-only engraftment, suggesting that intense myeloablation promotes erythropoiesis in this model (Figure 6C). Erythroid development in vivo was not inhibited by exposure to Dox possibly due to lower effective levels in tissues. Engraftment levels declined during extended transplantation. Low-level myeloid engraftment persisted 10–12 weeks posttransplant; however, erythroid cells were not detectable beyond 6 weeks (Figure S6C). These findings demonstrate that progenitors respecified from multiple hPSC lines mediate reproducible short-term engraftment.

(D) Colonies plated with or without Dox in the inducible transgene system. Erythroid and mixed colonies appear only upon Dox withdrawal. (Right) Representative images of CFU-GEMM, BFU-E, and CFU-GM colonies on plates without Dox.

(E) Self-renewing CD34$^+$ progenitors differentiate into myeloid and erythroid cells upon Dox removal. Flow analysis of dissociated *EARSM* colonies using the CD34 progenitor marker (left panels) and lineage markers CD11b and CD235a (right panel) is shown.

(F) Respecification of EB myeloid precursors into mixed lineage CFU-GEMM progenitors from MSC-IPS1 (left), CHB6-ESC (middle), and two other myeloid-restricted IPSC lines (right). EB progenitors were infected with *EARSM* and cultured with or without immobilized Delta1 ligand. Each group was plated with or without Dox.

(G) T cell potential of respecified cells in an OP9-DL1 stromal coculture. *EAR*-induced cells were cultured on OP9-DL1 without Dox (*EAR* − Dox), with Dox (*EAR* + Dox), or with Dox for the first 2 weeks followed by Dox removal (*EAR* switch). Development of CD4$^+$CD8$^+$ T cells was assessed following 35 days of culture, compared with CB CD34$^+$ cells. Plots are gated on CD45$^+$ cells.

Data in (B) and (F) are shown as mean ± SEM of at three independent replicates. See also Figures S4 and S5.

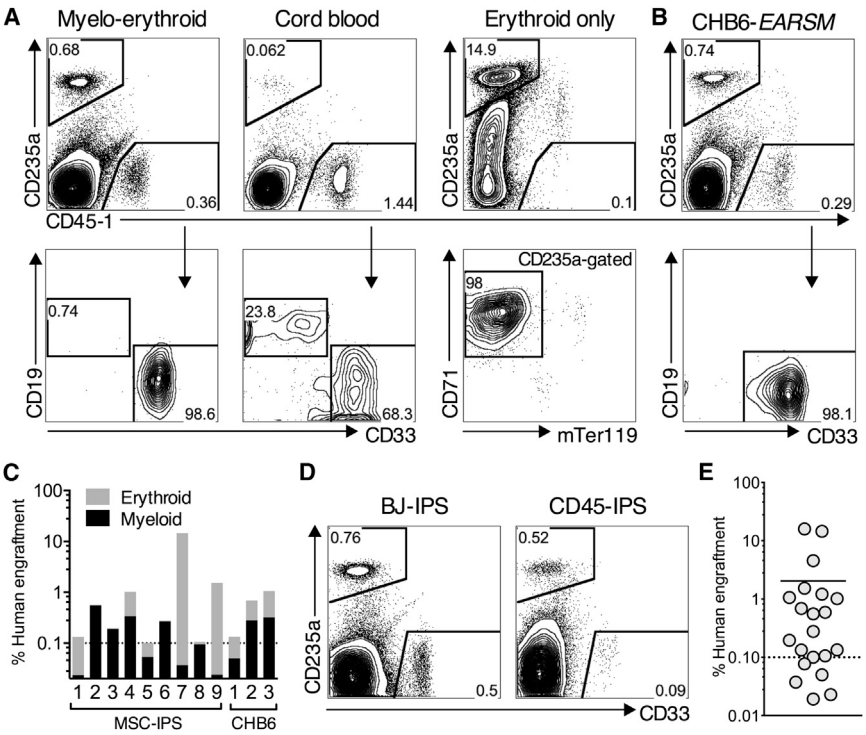

Figure 6. Short-Term Engraftment of Respecified Progenitors

EB progenitors derived from MSC-IPS (A) or CHB6-ESCs (B) were respecified with inducible *EARSM* for 7–16 days, and 0.8 to 1.2 × 10^6 cells were transplanted into the right femur of adult NSG mice. As a control, 1 × 10^6 CB mononuclear cells were transplanted. All mice received Dox in the drinking water. Human engraftment was analyzed 4–5 weeks posttransplantation using two human CD45 (myeloid, lymphoid) and CD235a (erythroid) antibodies. Only engraftment the injected femur is shown.

(A) Representative myelo-erythroid engraftment in *EARSM*- (left) and CB- (middle) transplanted mice. Cells positive for CD45 are subgated on CD19 and CD33 (bottom row). At right is a representative mouse engrafted only with human erythroid cells. $CD235a^+$ cells are subgated on CD71 and mouse Ter119.

(B) Representative engraftment in CHB6-ESC mice.

(C) Myeloid and erythroid lineage distribution in engrafted (>0.1% of human chimerism) MSC-IPS and CHB6-ESC mice. The height of the bar indicates total engraftment level calculated as % CD235a plus $\%CD45^+$.

(D) Representative engraftment in mice transplanted with independently-derived IPSC lines, BJ-IPS, and CD45-IPS.

(E) Summary of engraftment level in all transplanted mice with four different hPSC lines.

See also Figures S6 and S7.

To determine the basis for the beneficial effect of SOX4 and MYB on engraftment, we carried out expression profiling of $CD34^+CD38^-$ cells induced with the five factors. These samples clustered closely to *EAR*, indicating an overall similarity between all respecified progenitors (Figure S7A). Gene ontology categories for hematopoietic development and immune function were enriched among genes differentially regulated by *EARSM* relative to *EAR* (Figure S7B). *EAR* was associated with aberrant induction of a number of genes, such as heat-shock proteins (*HSPA6*) and Fcγ receptors (*FCGR2A*, *FCGR2B*, and *FCGR2C*) (Figure S7C). Repression of these transcripts by SOX4 and MYB may restore engraftment capacity of in vitro-specified cells.

Globin Switching during In Vivo Human Erythropoiesis

A pervasive feature of erythroid differentiation from hPSCs is the retention of embryonic and fetal patterns of globin expression (Chang et al., 2006; Dias et al., 2011). This property has been reported using independent protocols, suggesting that erythroid precursors fail to receive cues that promote proper developmental maturation reflected by globin gene switching (Anstee et al., 2012). Consistent with reported findings, BFU-Es isolated from $CD34^+CD45^+$ EBs expressed embryonic ε globin and fetal γ globin, but little or no adult β globin (Figure 7A). Respecification with *EARSM* did not alter this pattern of globin expression in vitro (Figure 7A). An important question that we sought to address is whether the adult bone marrow microenvironment could provide the cues to alter globin preference. To this end, we analyzed erythroid engraftment in *EARSM*-transplanted mice. Mouse erythrocytes were gated out with anti-mouse Ter119, showing that the majority of human erythrocytes were $CD235a^+CD71^+$ (Figure 7B). The marrow of cytopenic mice contained more $Ter119^+$ cells reflective of stress erythropoiesis, accompanied by progressive maturation of human erythrocytes (Figure 7B). The majority of sorted human $CD235a^+CD71^+$ cells were at the late erythroblast-normoblast stage of differentiation by morphology (Figure 7C) and marked by high levels of Band3 and low levels of CD49d (Figure 7D). Human erythrocytes do not readily enucleate in vivo; however, we detected some enucleated cells both by morphology and nuclear dye uptake (Figures 7C and 7D). Thus, hPSC-derived progenitors undergo erythroid maturation in vivo.

We next examined the pattern of hemoglobin expression in $CD235a^+CD71^+$ erythroblasts isolated from engrafted mice. Remarkably, ε globin was suppressed (4.0% of total globin, range 0.9%–7.1%), and β globin (12.6% of total globin, range 3.6%–28.1%) was induced, compared to cultured erythroblasts (Figure 7E). As expected, mice engrafted with CB expressed a mixture of γ and β globins. These findings were supported by analysis in single sorted $CD235a^+CD71^+$ cells. Single CB cells isolated from colonies or engrafted mice almost uniformly coexpressed γ and β globins (Figure 7F). Remarkably, 41.9% of *EARSM*-engrafted cells coexpressed γ and β globin, and a significant proportion (12.9%) expressed only β globin (Figure 7F). By comparison, adult globin-expressing cells were never detected in vitro (Figure 7F). The total levels of globin transcripts,

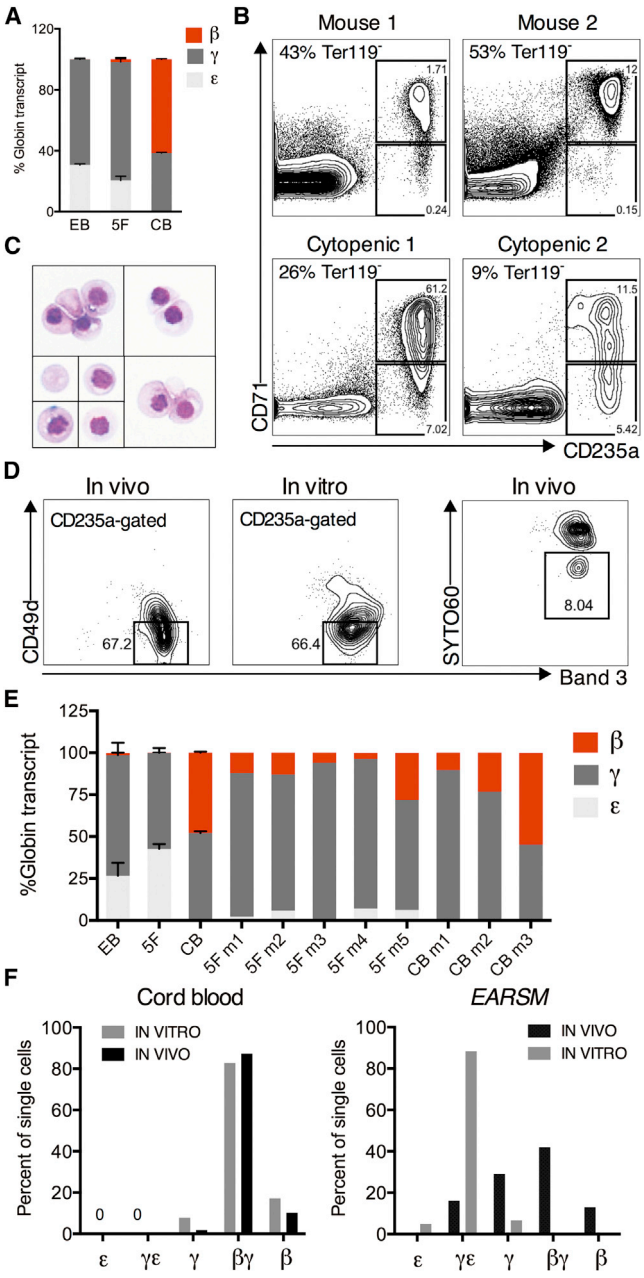

Figure 7. In Vivo Globin Switching in Embryonic Erythrocytes

(A) Quantitative PCR for the expression of adult *HBB* (β), fetal *HBG* (γ), and embryonic *HBE* (ε) hemoglobin genes in BFU-E colonies derived from EBs, *EARSM* (5F), and CB. Expression of each gene was calculated using absolute quantification and displayed as percent of total globin transcript.

(B) Analysis of human erythroid graft in two normopenic (Mouse 1 and 2) and two cytopenic *EARSM* mice using human CD71 and CD235a. Plots are subgated on Ter119$^-$ mouse cells, and the percent of mouse erythrocytes is indicated.

(C) Giemsa staining of Ter119$^-$CD71$^+$CD235$^+$ human erythrocytes. Representative single cells and clusters are shown.

(D) Erythroid maturation in vivo and in vitro determined by expression of Band3 and CD49d (integrin α4). Progressive maturation is marked by high levels of Band3 and loss of CD49d (gated population). Only CD235a$^+$ cells are shown. At right, the proportion of enucleated erythrocytes in vivo using cell-permeable nuclear dye SYTO60 (gated SYTO60$^-$ population) is shown.

(E) Hemoglobin expression in Ter119$^-$CD71$^+$CD235$^+$ human erythroblasts isolated from the marrow of multiple mice transplanted with CB or *EARSM* progenitors, in comparison with BFU-Es from EBs, 5F, and CB.

(F) Hemoglobin expression in single Ter119$^-$CD71$^+$CD235$^+$ erythroblasts isolated from transplanted mice (IN VIVO) or from cultured BFU-Es (IN VITRO). The cutoff for coexpression was set at 10% (i.e., a cell with 90%/10% ratio of β/γ transcript is classified as βγ, while 95%/5% is classified as β-only). Single-cell expression was validated by comparing against wells sorted with 50 cells.

Data in (A) and (E) are shown as the mean ± SEM of at least two samples. Data in (F) represents >80 sorted single cells.

and the degree of erythroid maturation as evidenced by Band3 and CD49d, were similar between cells isolated in vitro or in vivo (Figure 7D). These findings demonstrate that human IPSC-derived erythroid precursors respecified with transcription factors undergo hemoglobin switching in vivo, giving rise to definitive erythrocytes.

DISCUSSION

Generation of engraftable HSPCs from human pluripotent cells is a major goal in regenerative medicine. Here we report a significant advance toward this goal using a transcription-factor-mediated approach. In our system hPSCs are differentiated to hematopoietic progenitors and then transduced with a combination of HSC transcription factors that aim to respecify these progenitors to a stem cell fate. Using an in vitro screen to identify relevant combinations of factors, we demonstrate that HOXA9, ERG, and RORA convert myeloid-restricted precursors into self-renewing multilineage HSPCs with erythroid and lymphoid potential. These factors are sufficient to expand progenitors while maintaining a hierarchy with CD34$^+$CD38$^-$ "stem cells." HOXA9 and ERG can be further modified by SOX4 and MYB to enable short-term myelo-erythroid engraftment. These findings establish a transcription-factor-based system for engraftment from hPSCs that will serve as a platform for further improvements in transplantation potential.

The advent of IPSC technology has enabled the generation of pluripotent lines from patients with hematologic diseases. The hope has been that these lines can serve as models to gain insight into the molecular basis of these diseases and as platforms for drug screens (Cherry and Daley, 2013). However, the inability to generate large numbers of engraftable cells has precluded disease modeling in vivo, thereby limiting the scope of experiments and drug screens that can be performed. Our system described here may be suitable for modeling anemias and other red blood cell disorders due to its ability to generate large numbers of erythroid precursors in vitro, robust erythroid engraftment that can be enhanced by intensive myeloablation, and a high degree of hemoglobin maturation in vivo. Due to the near-unlimited capacity to produce erythroid cells, this transcription factor approach may also be suitable for transfusion-related applications (Migliaccio et al., 2012).

Erythroid precursors differentiated from hPSCs express embryonic and fetal, but not adult, hemoglobin (Chang et al., 2006). Induction of a switch to adult globin, critical for modeling thalassemias and sickle cell anemia caused by mutations in the HbB locus, has been the subject of intense investigation.

Silencing of embryonic and fetal globins is mediated by BCL11A, in tandem with KLF1, MYB, and others (Sankaran and Orkin, 2013; Sankaran et al., 2009). One possibility is that the expression or activity of these factors is not induced during hPSC differentiation in vitro resulting in the persistence of embryonic and fetal globins. The finding that erythrocytes in transplanted mice silence embryonic and induce adult globins supports the long-standing hypothesis that the bone marrow microenvironment can promote globin switching. This raises the possibility that globin switching is initiated by specific signaling pathways that activate BCL11A and other regulators following the migration of HSCs from FL to bone marrow after birth. The nature of these signals remains completely unknown. Since globin switching is regulated in a species-specific manner, transplantation of hPSC progenitors can serve as a model to interrogate the nature of the signaling interactions that drive globin switching (Sankaran et al., 2009).

Transcription factors that control stem cell state act as part of complex gene regulatory networks, and while these networks have been extensively modeled, functional studies have largely focused on the role of individual factors in controlling HSC fate (Orkin and Zon, 2008; Wilson et al., 2010). The respecification approach presents an opportunity to identify functional networks of cooperating factors. HOXA9 and ERG have been known to be required for HSC specification and expansion (Lawrence et al., 2005; Loughran et al., 2008). Both factors are also known oncogenes, and it is now well-established that normal self-renewal programs, if constitutively activated or dysregulated, can promote aberrant expansion of leukemic cells (Eppert et al., 2011). Our findings demonstrate that HOXA9, ERG, RORA, SOX4, and MYB are part of the same functional gene regulatory network. HOXA9 occupies *ERG*, *SOX4*, and *MYB* promoters, linking them on a molecular level (Huang et al., 2012). We propose that this network may have an important role in adult HSCs and leukemia-initiating cells. Our approach may provide deeper insights into the principles underlying the organization of HSC networks.

Current strategies for deriving HSPCs from heterologous cell types are based on directed differentiation from hPSCs or reprogramming of somatic cells (Pereira et al., 2013). We propose a hybrid strategy aiming to respecify HSCs from closely related progenitors by activating stem cell gene regulatory networks. However, respecification with our current factors has not achieved the major goal of generating a cell with long-term and multilineage repopulation potential. HSC state is controlled by a large number of transcription factors and epigenetic modifiers (Doulatov et al., 2012; Orkin and Zon, 2008). Powerful screening strategies are thus needed to identify rare combinations of cooperating factors. Our approach is based on detecting clonogenic progenitors arising as a result of self-renewal divisions in culture. However, these cell states may be incompatible with the in vivo requirements for HSC function. The alternative is to respecify directly in vivo to take advantage of the cues that normally support HSC self-renewal. However, only very rare combinations can likely be detected in this setting. The strategy we describe here provides a logical platform for pursuing both in vitro and in vivo screens aiming to reveal improved sets of factors that extend stem cell properties of respecified progenitors.

EXPERIMENTAL PROCEDURES

Details on colony assays, flow cytometry, microarray profiling, mouse transplantation, assessment of human cell engraftment, and quantitative and single-cell PCR are described in the Supplemental Experimental Procedures available online.

hPSC Culture

All experiments were performed with CHB6 ESC (NIH #0006) and MSC-IPS1 (Park et al., 2008). Human ESCs and IPSCs were maintained on mouse embryonic fibroblasts (GlobalStem) feeders in DMEM/F12 + 20% KnockOut-Serum Replacement (Invitrogen), 1 mM L-glutamine, 1 mM NEAA, 0.1 mM β-mercaptoethanol, and 10 ng/ml bFGF. Media was changed daily, and cells were passaged 1:4 onto fresh feeders every 7 days using standard clump passaging with collagenase IV.

EB Differentiation

EB differentiation was performed as previously described (Chadwick et al., 2003). Briefly, hPSC colonies were scraped into nonadherent rotating 10 cm plates. EB media was KO-DMEM + 20% FBS (Stem Cell Technologies), 1 mM L-glutamine, 1 mM NEAA, penicillin/streptomycin, 0.1 mM β-mercaptoethanol, 200 μg/ml h-transferrin, and 50 μg/ml ascorbic acid. After 24 hr, media was changed by allowing EBs to settle by gravity and replacing with EB media supplemented with growth factors as follows: 50 ng/ml BMP4 (R&D Systems), 300 ng/ml SCF, 300 ng/ml FLT3, 50 ng/ml G-CSF, 20 ng/ml IL-6, 10 ng/ml IL-3 (all Peprotech). Media was changed on day 5 and day 10. EBs were dissociated on day 14 by digestion with collagenase B (Roche) for 2 hr and by treatment with enzyme-free dissociation buffer (GIBCO), then filtered through an 80 μm filter. Dissociated EBs were frozen in 10% DMSO and 40% FBS freezing solution.

Lentivirus Production

Plasmids for the 9F library were obtained as Gateway plasmids (GeneCopoeia). Open reading frames were cloned into lentiviral vectors using LR Clonase (Invitrogen). Two vectors were used, pSMAL-GFP (constitutive) and pINDUCER-21 (Meerbrey et al., 2011). Lentiviral particles were produced by transfecting 293T-17 cells (ATCC) with the third-generation packaging plasmids. Virus was harvested 12 and 36 hr after transfection and concentrated by ultracentrifugation at 23,000 rpm for 2 hr. Constructs were titered by serial dilution on 293T cells.

Progenitor Sorting

Dissociated EB cells were thawed following the Lonza Poietics protocol (http://bio.lonza.com/uploads/tx_mwaxmarketingmaterial/Lonza_ManualsProductInstructions_Procedure_for_Thawing_Poietics_Cells.pdf) and resuspended at 1 × 10^6 per 100 μl staining buffer (PBS + 2% FBS). Cells were stained with a 1:50 dilution of CD45 PE-Cy5 (Immu19.2; Clontech), CD34 PE-Cy7 (8G12; BD), and DAPI for 20 min at room temperature. All sorting was performed on a BD FACS Aria II cell sorter using a 70 μm nozzle.

Lentiviral Gene Transfer

Sorted $CD34^+CD45^+$ progenitors were seeded on fibronectin-coated (10 μg/cm^2) 96-well plates at a density of 2 to 5 × 10^4 cells per well. The infection media was IMDM + 20% BIT (StemCell Technologies), 1 mM L-glutamine, and 0.1 mM β-mercaptoethanol, with 300 ng/ml SCF, 300 ng/ml FLT3, 50 ng/ml G- CSF, 20 ng/ml IL6, and 10 ng/ml IL3 (all Peprotech). Lentiviral infections were carried out in a total volume of 150 μl. The multiplicity of infection for the factors was as follows: 9F 20, ERG 5.0, HOXA9 5.0, RORA 3.0, SOX4 3.0, and MYB 3.0. Virus was concentrated onto cells by centrifuging the plate at 2,500 rpm for 30 min at room temperature. Infections were carried out for 24–36 hr.

Progenitor Culture

Following gene transfer, progenitors were cultured in suspension in infection media supplemented with 50 ng/ml SCF, 50 ng/ml FLT3, 50 ng/ml TPO, 50 ng/ml IL6, and 10 ng/ml IL3 (all R&D Systems). To standardize these conditions, for all experiments with inducible constructs (including all transplantation experiments), infection media was replaced with StemSpan SFEM

(StemCell Technologies). Dox was added at 2 μg/ml (Sigma). For culturing on immobilized ligands, nontissue culture plates were coated with 2.5 μg/ml Delta1 extIgG and 5 μg/ml recombinant human retronectin (CH296, Takara Bio) for 2 hr at 37°C. Culture media was same as above. Cultures were maintained at a density of $<1 \times 10^6$ cells/ml, and media was changed every 3–4 days.

ACCESSION NUMBERS

Microarray data from this study has been deposited to GEO database under accession number GSE49938.

SUPPLEMENTAL INFORMATION

Supplemental Information for this article includes Supplemental Experimental Procedures, seven figures, and four tables and can be found with this article online at http://dx.doi.org/10.1016/j.stem.2013.09.002.

ACKNOWLEDGMENTS

The authors would like to thank Thorsten Schlaeger and the BCH ESC core, Ronald Mathieu from the flow cytometry core, and Norman Gerry from the Coriell Genotyping and Microarray Center for assistance. Andrea Ditadi and Gordon Keller provided reagents and advice. Band3 antibody was a gift from the Narla Mohandas lab. This work is supported by grants from the US National Institute of Diabetes and Digestive and Kidney Diseases (R24-DK092760) and the National Heart, Lung, Blood Institute Progenitor Cell Biology Consortium (UO1-HL100001); Alex's Lemonade Stand; and the Doris Duke Medical Foundation. G.Q.D. is an associate member of the Broad Institute and an investigator of the Howard Hughes Medical Institute and the Manton Center for Orphan Disease Research. S.D. is supported by a fellowship from the Helen Hay Whitney Foundation. L.T.V. is supported by the NSF Graduate Research Fellowship.

Received: July 9, 2013
Revised: August 20, 2013
Accepted: September 6, 2013
Published: October 3, 2013

REFERENCES

Agarwal, S., Loh, Y.H., McLoughlin, E.M., Huang, J., Park, I.H., Miller, J.D., Huo, H., Okuka, M., Dos Reis, R.M., Loewer, S., et al. (2010). Telomere elongation in induced pluripotent stem cells from dyskeratosis congenita patients. Nature *464*, 292–296.

Amsellem, S., Pflumio, F., Bardinet, D., Izac, B., Charneau, P., Romeo, P.H., Dubart-Kupperschmitt, A., and Fichelson, S. (2003). Ex vivo expansion of human hematopoietic stem cells by direct delivery of the HOXB4 homeoprotein. Nat. Med. *9*, 1423–1427.

Anstee, D.J., Gampel, A., and Toye, A.M. (2012). Ex-vivo generation of human red cells for transfusion. Curr. Opin. Hematol. *19*, 163–169.

Bertrand, J.Y., Chi, N.C., Santoso, B., Teng, S., Stainier, D.Y., and Traver, D. (2010). Haematopoietic stem cells derive directly from aortic endothelium during development. Nature *464*, 108–111.

Boisset, J.C., van Cappellen, W., Andrieu-Soler, C., Galjart, N., Dzierzak, E., and Robin, C. (2010). In vivo imaging of haematopoietic cells emerging from the mouse aortic endothelium. Nature *464*, 116–120.

Chadwick, K., Wang, L., Li, L., Menendez, P., Murdoch, B., Rouleau, A., and Bhatia, M. (2003). Cytokines and BMP-4 promote hematopoietic differentiation of human embryonic stem cells. Blood *102*, 906–915.

Chambers, S.M., Boles, N.C., Lin, K.Y., Tierney, M.P., Bowman, T.V., Bradfute, S.B., Chen, A.J., Merchant, A.A., Sirin, O., Weksberg, D.C., et al. (2007). Hematopoietic fingerprints: an expression database of stem cells and their progeny. Cell Stem Cell *1*, 578–591.

Chang, K.H., Nelson, A.M., Cao, H., Wang, L., Nakamoto, B., Ware, C.B., and Papayannopoulou, T. (2006). Definitive-like erythroid cells derived from human embryonic stem cells coexpress high levels of embryonic and fetal globins with little or no adult globin. Blood *108*, 1515–1523.

Cherry, A.B., and Daley, G.Q. (2013). Reprogrammed cells for disease modeling and regenerative medicine. Annu. Rev. Med. *64*, 277–290.

Cherry, A.B., Gagne, K.E., McLoughlin, E.M., Baccei, A., Gorman, B., Hartung, O., Miller, J.D., Zhang, J., Zon, R.L., Ince, T.A., et al. (2013). Induced pluripotent stem cells with a mitochondrial DNA deletion. Stem Cells *31*, 1287–1297.

Choi, K.D., Vodyanik, M.A., Togarrati, P.P., Suknuntha, K., Kumar, A., Samarjeet, F., Probasco, M.D., Tian, S., Stewart, R., Thomson, J.A., et al. (2012). Identification of the hemogenic endothelial progenitor and its direct precursor in human pluripotent stem cell differentiation cultures. Cell Reports *2*, 553–567.

Delaney, C., Varnum-Finney, B., Aoyama, K., Brashem-Stein, C., and Bernstein, I.D. (2005). Dose-dependent effects of the Notch ligand Delta1 on ex vivo differentiation and in vivo marrow repopulating ability of cord blood cells. Blood *106*, 2693–2699.

Di-Poï, N., Koch, U., Radtke, F., and Duboule, D. (2010). Additive and global functions of HoxA cluster genes in mesoderm derivatives. Dev. Biol. *341*, 488–498.

Dias, J., Gumenyuk, M., Kang, H., Vodyanik, M., Yu, J., Thomson, J.A., and Slukvin, I.I. (2011). Generation of red blood cells from human induced pluripotent stem cells. Stem Cells Dev. *20*, 1639–1647.

Doulatov, S., Notta, F., Eppert, K., Nguyen, L.T., Ohashi, P.S., and Dick, J.E. (2010). Revised map of the human progenitor hierarchy shows the origin of macrophages and dendritic cells in early lymphoid development. Nat. Immunol. *11*, 585–593.

Doulatov, S., Notta, F., Laurenti, E., and Dick, J.E. (2012). Hematopoiesis: a human perspective. Cell Stem Cell *10*, 120–136.

Eppert, K., Takenaka, K., Lechman, E.R., Waldron, L., Nilsson, B., van Galen, P., Metzeler, K.H., Poeppl, A., Ling, V., Beyene, J., et al. (2011). Stem cell gene expression programs influence clinical outcome in human leukemia. Nat. Med. *17*, 1086–1093.

Garçon, L., Ge, J., Manjunath, S.H., Mills, J.A., Apicella, M., Parikh, S., Sullivan, L.M., Podsakoff, G.M., Gadue, P., French, D.L., et al. (2013). Ribosomal and hematopoietic defects in induced pluripotent stem cells derived from Diamond Blackfan anemia patients. Blood *122*, 912–921.

Hu, Z., Van Rooijen, N., and Yang, Y.G. (2011). Macrophages prevent human red blood cell reconstitution in immunodeficient mice. Blood *118*, 5938–5946.

Huang, Y., Sitwala, K., Bronstein, J., Sanders, D., Dandekar, M., Collins, C., Robertson, G., MacDonald, J., Cezard, T., Bilenky, M., et al. (2012). Identification and characterization of Hoxa9 binding sites in hematopoietic cells. Blood *119*, 388–398.

Ivanova, N.B., Dimos, J.T., Schaniel, C., Hackney, J.A., Moore, K.A., and Lemischka, I.R. (2002). A stem cell molecular signature. Science *298*, 601–604.

Kennedy, M., Awong, G., Sturgeon, C.M., Ditadi, A., LaMotte-Mohs, R., Zuniga-Pflucker, J.C., and Keller, G. (2012). T lymphocyte potential marks the emergence of definitive hematopoietic progenitors in human pluripotent stem cell differentiation cultures. Cell Reports *2*, 1722–1735.

Kumano, K., Arai, S., Hosoi, M., Taoka, K., Takayama, N., Otsu, M., Nagae, G., Ueda, K., Nakazaki, K., Kamikubo, Y., et al. (2012). Generation of induced pluripotent stem cells from primary chronic myelogenous leukemia patient samples. Blood *119*, 6234–6242.

Kyba, M., Perlingeiro, R.C., and Daley, G.Q. (2002). HoxB4 confers definitive lymphoid-myeloid engraftment potential on embryonic stem cell and yolk sac hematopoietic progenitors. Cell *109*, 29–37.

Laurenti, E., Doulatov, S., Zandi, S., Plumb, I., Chen, J., April, C., Fan, J.B., and Dick, J.E. (2013). The transcriptional architecture of early human hematopoiesis identifies multilevel control of lymphoid commitment. Nat. Immunol. *14*, 756–763.

Lawrence, H.J., Christensen, J., Fong, S., Hu, Y.L., Weissman, I., Sauvageau, G., Humphries, R.K., and Largman, C. (2005). Loss of expression of the Hoxa-9 homeobox gene impairs the proliferation and repopulating ability of hematopoietic stem cells. Blood *106*, 3988–3994.

Ledran, M.H., Krassowska, A., Armstrong, L., Dimmick, I., Renström, J., Lang, R., Yung, S., Santibanez-Coref, M., Dzierzak, E., Stojkovic, M., et al. (2008). Efficient hematopoietic differentiation of human embryonic stem cells on stromal cells derived from hematopoietic niches. Cell Stem Cell *3*, 85–98.

Lee, G.S., Kim, B.S., Sheih, J.H., and Moore, M. (2008). Forced expression of HoxB4 enhances hematopoietic differentiation by human embryonic stem cells. Mol. Cells *25*, 487–493.

Loughran, S.J., Kruse, E.A., Hacking, D.F., de Graaf, C.A., Hyland, C.D., Willson, T.A., Henley, K.J., Ellis, S., Voss, A.K., Metcalf, D., et al. (2008). The transcription factor Erg is essential for definitive hematopoiesis and the function of adult hematopoietic stem cells. Nat. Immunol. *9*, 810–819.

Martin, C.H., Woll, P.S., Ni, Z., Zúñiga-Pflücker, J.C., and Kaufman, D.S. (2008). Differences in lymphocyte developmental potential between human embryonic stem cell and umbilical cord blood-derived hematopoietic progenitor cells. Blood *112*, 2730–2737.

Mazurier, F., Doedens, M., Gan, O.I., and Dick, J.E. (2003). Rapid myeloerythroid repopulation after intrafemoral transplantation of NOD-SCID mice reveals a new class of human stem cells. Nat. Med. *9*, 959–963.

McKinney-Freeman, S., Cahan, P., Li, H., Lacadie, S.A., Huang, H.T., Curran, M., Loewer, S., Naveiras, O., Kathrein, K.L., Konantz, M., et al. (2012). The transcriptional landscape of hematopoietic stem cell ontogeny. Cell Stem Cell *11*, 701–714.

Meerbrey, K.L., Hu, G., Kessler, J.D., Roarty, K., Li, M.Z., Fang, J.E., Herschkowitz, J.I., Burrows, A.E., Ciccia, A., Sun, T., et al. (2011). The pINDUCER lentiviral toolkit for inducible RNA interference in vitro and in vivo. Proc. Natl. Acad. Sci. USA *108*, 3665–3670.

Migliaccio, A.R., Whitsett, C., Papayannopoulou, T., and Sadelain, M. (2012). The potential of stem cells as an in vitro source of red blood cells for transfusion. Cell Stem Cell *10*, 115–119.

Müller, L.U., Milsom, M.D., Harris, C.E., Vyas, R., Brumme, K.M., Parmar, K., Moreau, L.A., Schambach, A., Park, I.H., London, W.B., et al. (2012). Overcoming reprogramming resistance of Fanconi anemia cells. Blood *119*, 5449–5457.

Notta, F., Doulatov, S., Laurenti, E., Poeppl, A., Jurisica, I., and Dick, J.E. (2011). Isolation of single human hematopoietic stem cells capable of long-term multilineage engraftment. Science *333*, 218–221.

Novershtern, N., Subramanian, A., Lawton, L.N., Mak, R.H., Haining, W.N., McConkey, M.E., Habib, N., Yosef, N., Chang, C.Y., Shay, T., et al. (2011). Densely interconnected transcriptional circuits control cell states in human hematopoiesis. Cell *144*, 296–309.

Orkin, S.H., and Zon, L.I. (2008). Hematopoiesis: an evolving paradigm for stem cell biology. Cell *132*, 631–644.

Park, I.H., Zhao, R., West, J.A., Yabuuchi, A., Huo, H., Ince, T.A., Lerou, P.H., Lensch, M.W., and Daley, G.Q. (2008). Reprogramming of human somatic cells to pluripotency with defined factors. Nature *451*, 141–146.

Pereira, C.F., Chang, B., Qiu, J., Niu, X., Papatsenko, D., Hendry, C.E., Clark, N.R., Nomura-Kitabayashi, A., Kovacic, J.C., Ma'ayan, A., et al. (2013). Induction of a hemogenic program in mouse fibroblasts. Cell Stem Cell *13*, 205–218.

Sankaran, V.G., and Orkin, S.H. (2013). The switch from fetal to adult hemoglobin. Cold Spring Harbor Perspectives in Medicine *3*, a011643.

Sankaran, V.G., Xu, J., Ragoczy, T., Ippolito, G.C., Walkley, C.R., Maika, S.D., Fujiwara, Y., Ito, M., Groudine, M., Bender, M.A., et al. (2009). Developmental and species-divergent globin switching are driven by BCL11A. Nature *460*, 1093–1097.

Tulpule, A., Kelley, J.M., Lensch, M.W., McPherson, J., Park, I.H., Hartung, O., Nakamura, T., Schlaeger, T.M., Shimamura, A., and Daley, G.Q. (2013). Pluripotent stem cell models of Shwachman-Diamond syndrome reveal a common mechanism for pancreatic and hematopoietic dysfunction. Cell Stem Cell *12*, 727–736.

Wang, L., Menendez, P., Shojaei, F., Li, L., Mazurier, F., Dick, J.E., Cerdan, C., Levac, K., and Bhatia, M. (2005). Generation of hematopoietic repopulating cells from human embryonic stem cells independent of ectopic HOXB4 expression. J. Exp. Med. *201*, 1603–1614.

Wilson, N.K., Foster, S.D., Wang, X., Knezevic, K., Schütte, J., Kaimakis, P., Chilarska, P.M., Kinston, S., Ouwehand, W.H., Dzierzak, E., et al. (2010). Combinatorial transcriptional control in blood stem/progenitor cells: genome-wide analysis of ten major transcriptional regulators. Cell Stem Cell *7*, 532–544.

Ye, Z., Zhan, H., Mali, P., Dowey, S., Williams, D.M., Jang, Y.Y., Dang, C.V., Spivak, J.L., Moliterno, A.R., and Cheng, L. (2009). Human-induced pluripotent stem cells from blood cells of healthy donors and patients with acquired blood disorders. Blood *114*, 5473–5480.

Zou, J., Mali, P., Huang, X., Dowey, S.N., and Cheng, L. (2011). Site-specific gene correction of a point mutation in human iPS cells derived from an adult patient with sickle cell disease. Blood *118*, 4599–4608.